

# Elasto-Plastic Transient Dynamic Response of Tubular Section Steel Cantilever Beam under Impact Loading

Ali Al Aloosi<sup>1</sup> and Zia Razzaq<sup>2</sup>

<sup>1</sup> Old Dominion University

*Received: 5 April 2016 Accepted: 30 April 2016 Published: 15 May 2016*

---

## Abstract

This paper presents the outcome of an experimental and theoretical investigation into the loadcarrying capacity of Fiber Reinforced Polymer (FRP) I-section beams subjected to four-point loading. The overall lateral-torsional buckling, web and flange local buckling as well as material rupture load estimates are also made using the American Society of Civil Engineers' Load and Resistance Factor Design (ASCELRFD) Pre-Standard for FRP Structures. Lateral-torsional buckling failure mode is found to govern for each of the beams studied. The study also revealed that the height of applied loads relative to the shear center has a very significant influence on lateral-torsional buckling load of a beam thus making ASCELRFD buckling load estimates over-conservative in a variety of cases.

---

*Index terms*— impact, dynamic, elasto-plastic, flexural dynamic equilibrium.

## 1 I. Introduction

azzaq et al. [1] conducted a theoretical and experimental study of slender tubular columns with partial rotational end restraints in the presence of initial imperfections. New explicit formulas and finite-difference formulation were derived for predicting the elastic buckling load and predicting the natural frequency. Jones [2] studied the behavior of fully clamped beams when struck at the mid-span by a rigid mass and compared it with the corresponding exact theoretical predictions of dynamic rigid-plastic analyses. Wen et al. [3] proposed a quasi-static procedure based on the principle of virtual work for estimating the dynamic plastic response and failure of clamped metal beams subjected to a low velocity impact at any point on the span by a heavy mass. The paper by Zeinoddini et al [4] described experimental studies in which axially pre-loaded tubes were examined under lateral dynamic impact loads. The tubes were impacted by a dropped object with a velocity of about 7 meter/sec at their midspan.

The current paper presents the outcome of an experimental and theoretical study of a partially end restrained cantilever beam under impact loading. New terms are added to the governing dynamic equilibrium equation for the problem to account for elasto-plastic effects when transient dynamic response of the cantilever needs to be predicted. Numerical results are obtained using an iterative finite-difference procedure. The iterative solution process also involves a materially nonlinear tangent stiffness method to deal with cross-sectional plastification as a function of time.

## 2 II. Experimental Study

Figure ?? shows schematic of a cantilever beam QB subjected to a forcing function  $F(t)$  generated by a freely falling impact load. For the beam, the origin of the longitudinal ordinate  $z$  is at Q. At end B, the cantilever beam is attached to a rotationally flexible elastic support simulated as a rotational spring having a rotational spring constant value of  $k_B = 6 \times 10^6$  kip-in/rad. The cantilever beam QB has a length  $L$  of 33 in. and a  $2 \times 2 \times 0.125$  in. hollow square cross section. The test setup is shown in Figure ?. The impact tests were performed using three different impactors numbered 1, 2, and 3 weighing 60 lb., 140 lb., and 400 lb., respectively. Each impactor had an accelerometer inside a steel chamber attached at the impactor bottom end to record acceleration-time

relationship which was curve-fitted using a quadratic function of time t. The relationships marked C1-1, C1-2, and C1-3 shown in Figure 3 correspond to Impactors 1, 2, and 3 each dropped onto the cantilever beam with a gap of one inch between the cantilever beam's top surface and the bottom face of the steel chamber. In the same figure, the relationship marked C1-4 is for Impactor 3 dropped with a gap of two inches. The forcing function F(t) is generated by multiplying the ordinate of Figure 3 by mg, where m is the impactor mass and g is 32.2 ft./sec<sup>2</sup>. The forcing functions for Impactors 1, 2, and 3 when dropped from 1 inch height are as follow: F<sub>2</sub>(t) = (-

The forcing function for Impactor 3 when dropped from 2 inches height is as follows: F<sub>4</sub>(t) = (-804.63 t<sup>2</sup> + 111.12 t - 1.4058) mg for 0.008 ≤ t ≤ 0.125 (4)

The lower limit represents the time when the impactor hits the cantilever beam tip while the upper limit represents the time when the impactor is detached from the beam.

Global Journal of Researches in Engineering ( ) Volume XVI Issue V Version I F<sub>1</sub>(t) = (-6338.8 t<sup>2</sup> + 418.56 t - 3.0877) mg for 0.008 ≤ t ≤ 0.057 (1) Three strain gauges were installed on the cantilever beam to measure strain-time histories. The strain gauges, designated as SG1, SG2, and SG3, were installed on the cantilever beam at three locations at a distance of one inch from end B as shown in Figure 4.

### 3 III. Theoretical Study

The elastic dynamic flexural equilibrium equation for a beam without damping is given in the literature [5] as follows:  $EI \frac{\partial^4 w}{\partial z^4} + \rho A \frac{\partial^2 w}{\partial t^2} = F(t)$  (5)

in which EI is the elastic flexural rigidity, w is the beam deflection, m is the beam mass per unit length, z is the horizontal distance along the member, t is the time, and F(t) is a forcing function. In the inelastic range, EI changes with the applied load. Therefore, the inelastic partial differential equation of motion can be expressed as:  $E_p \frac{\partial^4 w}{\partial z^4} + \rho A \frac{\partial^2 w}{\partial t^2} = F(t)$  (6)

where E<sub>p</sub> is the elasto-plastic flexural rigidity. In this equation, damping is not included since it is negligible due to the predominant influence of impact loading on the beam response for the duration of the impact. For a given time t, E<sub>p</sub> is a function of z, thus Equation 6 becomes:  $E_p(z) \frac{\partial^4 w}{\partial z^4} + \rho A \frac{\partial^2 w}{\partial t^2} = F(t)$  (7)

To obtain the numerical results presented in this paper, the first and second partial derivatives of w appearing in Equation 7 were iteratively generated with Lagrangian polynomials along the z axis.

#### 4 a) Boundary Conditions

At Q in Figure ??, the bending moment is zero, thus:  $M(z=0, t) = 0$  (8a)

The shear force at Q can be expressed as:  $V(z=0, t) = 0$  (8b)

At end B, the cantilever beam has no vertical movement:  $w(z=L, t) = 0$  (8c)

The elastic moment-rotation relationship of the rotational spring at B is expressed as:  $M_B = k_B \theta_B$  (8d)

Where k<sub>B</sub> is the stiffness of the rotational spring at end B, and θ<sub>B</sub> is the rotation of the cantilever beam at the same location. Since θ<sub>B</sub> is the first derivative of the deflection at end B, thus:  $\theta_B = \frac{\partial w}{\partial z}(z=L, t)$  (8e)

The minus sign in this equation is consistent with downward deflections taken as positive in the derivation of Equation 7. The boundary conditions presented above are used in the elasto-plastic dynamic analysis of the cantilever beam.

#### 5 b) Initial Conditions

The initial conditions for the problem are:  $w(z, 0) = 0$  (9a)  $\dot{w}(z, 0) = 0$  (9b)

The initial condition given by Equation 9a states that at time t equal zero, the deflection is zero. Equation 9b states that the initial velocity is zero.

#### 6 c) Finite-Difference Solution

Central finite-difference expressions [6] were used to solve Equation 7 with boundary and initial conditions presented in Sections 3.1 and 3.2. A total of N panels were used for the cantilever beam over the interval (0, L) involving nodes i = 1, 2, 3, ..., (N+1). The finite-difference scheme also results in 'phantom points' outside of the interval (0,L) and are accounted-for in the solution algorithm. Using second order finite-difference expressions, Equation 7 can be written as:  $\frac{w_{i+1} - 2w_i + w_{i-1}}{\Delta z^2} + \rho A \frac{w_{i,j+1} - 2w_{i,j} + w_{i,j-1}}{\Delta t^2} = F_{i,j}$  (10)

in which, Δz is the panel length along the z-axis of the sub-assembly, and Δt is the time interval. The subscript i refers to the ith nodal point over the domain 0 < z < L, and the subscript j refers to the number of time increments such that the time at t<sub>j</sub> is given by the following equation: t<sub>j</sub> = j(Δt), for each j=0, 1, 2, 3, ...

Similarly, the boundary conditions 8a, 8b, 8c, and 8d can be expressed in finite-difference form as follows:  $w_0 = 0$  (11a)  $\dot{w}_0 = 0$  (11b)  $w_N = 0$  (11c)  $\dot{w}_N = 0$  (11d)

---

100  $u_{i+1} = 0$  (11b)  $u_i + 1 = 0$  (11c)  $u_i + u_{i+1} = 0$  (11d)

101  
102 Applying Equation 10 at  $i=1, 2, 3, \dots, N$ , and invoking conditions 11a, 11b, 11c, and 11d leads to the following  
103 matrix equation:  $[K] \{u\} = \{F\}$  (12) in which  $[K]$   
104  $[K] = [K_1, K_2, \dots, K_N]$  (13a)  $[K_1] = [K_2] = \dots = [K_N]$  (13b)  $[K_1] = [K_2] = \dots = [K_N]$  (13c)

105 The  $[K]$  coefficient matrix is symmetric and of the order  $N \times N$ .

106 A finite-difference iterative algorithm was developed for the nonlinear dynamic analysis of the cantilever beam.  
107 The deflections along the cantilever beam were found for the first time increment using the elastic formula. To  
108 avoid having a negative time interval due to the use of central finite-difference, a start-up equation [1] was used  
109 to initialize the process. Initial nodal deflections were found using Equation 10. An iterative tangent stiffness  
110 procedure was utilized to compute the curvatures due to the applied moments which satisfied cross-sectional  
111 equilibrium. Next, the elasto-plastic cross-sectional properties were calculated using the computed curvatures,  
112 and Revised deflections were found using the updated cross-sectional properties. The revised deflections were  
113 compared with the initial deflections for the same time increment. If the difference was found to be larger than a  
114 specified tolerance value, another iteration was performed for that time increment. If the difference was found to  
115 be smaller than a tolerance value, the procedure was continued to the next time increment with the corresponding  
116 new value of the forcing function. This solution procedure was used to generate the theoretical strain-time  
117 curves shown in Figures 5 through 12.

## 118 7 d) Cantilever Behavior under Impact Loading

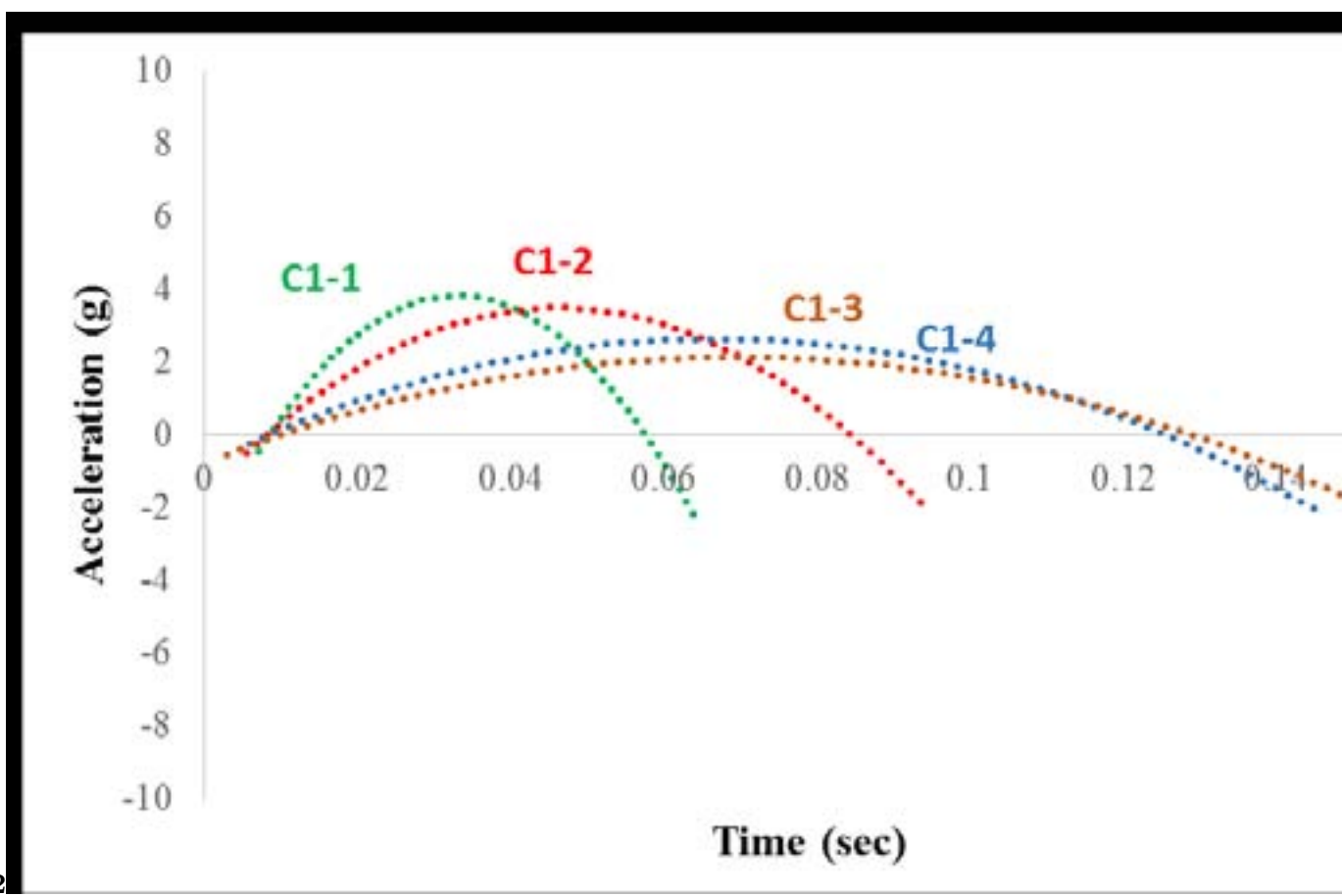
119 Table 1 compares the maximum experimental and theoretical moments at section B of the cantilever beam for  
120 Tests C1-1, C1-2, C1-3, and C1-4. For Test C1-1, Impactor 1 was dropped from one inch above end Q of the  
121 cantilever beam. Figures 5 and 6 show theoretical and experimental strain-time curves for SG1 and SG2,  
122 respectively. Both figures show the same trending, and the peak values agreed well. The ratios between the  
123 tested to the predicted strain results ranged from 0.99 to 1.17.

124 Table 2 shows the experimental and the theoretical strains, and their comparison. For this test, the  
125 experimental maximum moment at section B was 10.8 kip-in. and the theoretical value was 9.4 kip-in. The  
126 difference between the theoretical and the experimental results was 15%. The experimental and the theoretical  
127 moment values were in good agreement and they were in the elastic range. For Test C1-2, Impactor 2 was dropped  
128 from one inch above end Q of the cantilever beam. Figures 7 and 8 show the theoretical and the experimental  
129 strain-time curves for SG1 and SG2, respectively. Table 3 shows the experimental and the theoretical strains and,  
130 their comparison. The ratios between the tested to the predicted strain results ranged from 0.93 to 1.01. For this  
131 test, the experimental maximum moment at section B was 20.3 kip-in and the theoretical value was 17.8 kip-in.  
132 The difference between the theoretical and the experimental results was 14%. A good agreement was reached  
133 between the tested and the predicted results. Results from this test were in the elastic range. For Test C1-3,  
134 Impactor 3 was dropped from one inch above end Q of the cantilever. Figures 9 and 10 show the theoretical  
135 and the experimental strain-time curves for SG1 and SG2, respectively. Table 4 shows the experimental and the  
136 theoretical strains and, their comparison. The ratios between the tested to the predicted strain results ranged  
137 from 0.89 to 0.86, which are considered to be reasonable results. There was an overall good agreement in the  
138 shape of all the load-strain curves. For this test, the experimental maximum moment at section B was 38.1 kip-in  
139 and the theoretical value was 37.7 kip-in. The difference between the theoretical and the experimental results  
140 was 2%. Both the experimental and the theoretical curves were very similar and their peak values were very  
141 close. This test caused partial plastification on the cantilever beam. For Test C1-4, Impactor 3 was dropped  
142 from two inches above end Q of the cantilever. Figures 11 and 12 show the theoretical and the experimental  
143 strain-time curves for SG1 and SG2, respectively. Table 5 shows the experimental and theoretical strains, and  
144 their comparison. The ratios between the tested to the predicted strain results ranged from 1.01 to 1.06. For this  
145 test, the experimental maximum moment at section B was 39.5 kip-in and the theoretical value was 39.2 kip-in.  
146 Both the theoretical and the experimental results showed the formation of a plastic hinge at section B. It can be  
147 seen that there was good agreement between the predicted and the experimental values for the strains and the  
148 moments.

## 149 8 Global

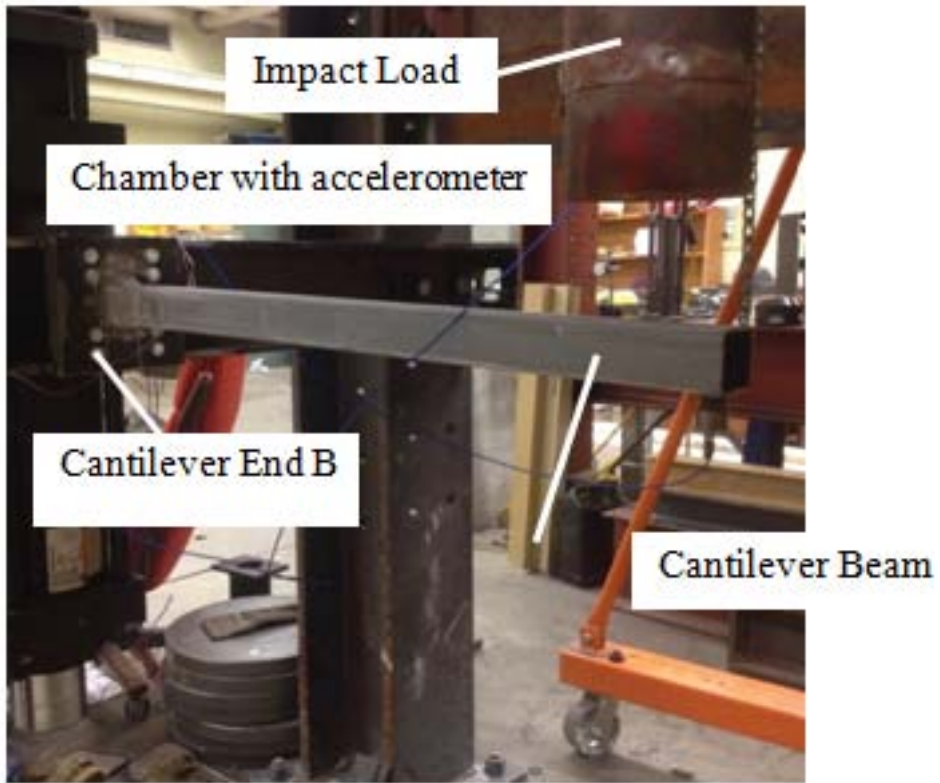
## 150 9 Conclusion

151 A theoretical and experimental study of the dynamic elasto-plastic behavior of a steel cantilever beam is presented.  
152 A mathematical model based on a partial differential equation of inelastic dynamic equilibrium is successfully  
153 developed including new terms to account for elasto-plastic behavior of a steel cantilever beam. The iterative  
154 finite-difference solution algorithm predicted experimental elasto-plastic behavior of the cantilever beam for  
155 various impact forcing functions. It was also found that the weight of the impactor is directly related to the total  
156 duration of impact. By comparing the curve-fitted acceleration response generated by different impactors, it was



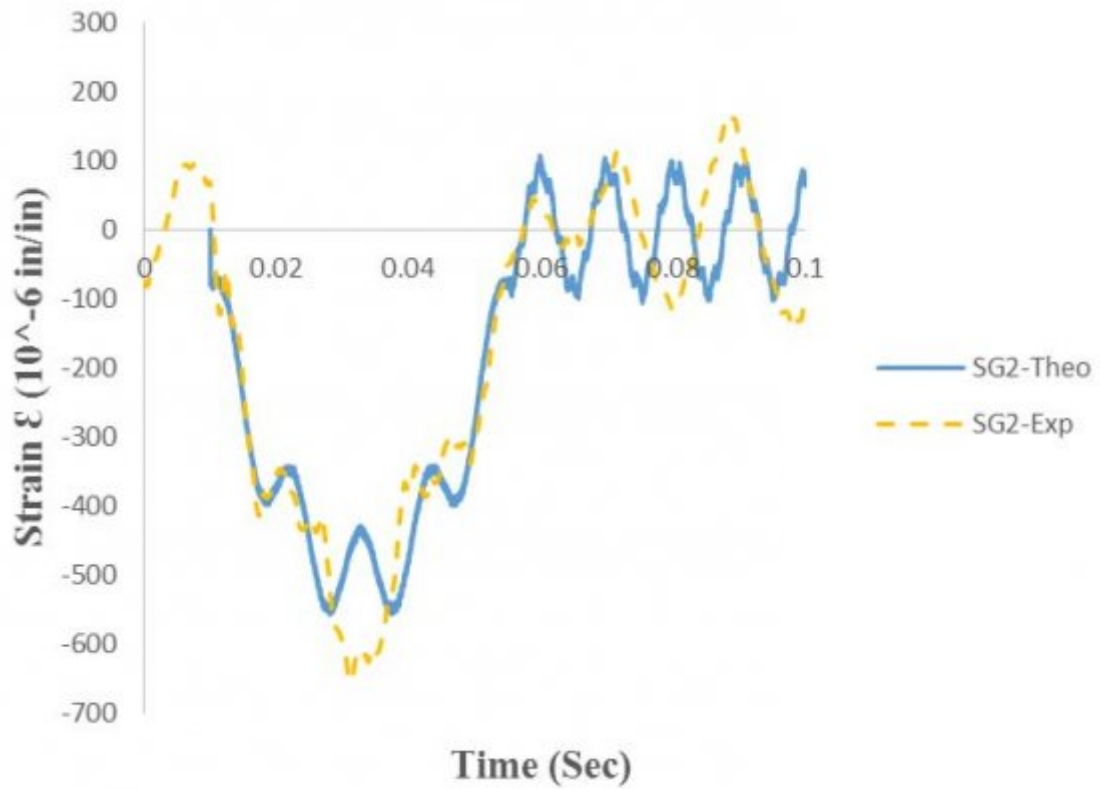
12

Figure 1: Figure 1 :Figure 2 :



3

Figure 2: Figure 3 :



4

Figure 3: Figure 4 :

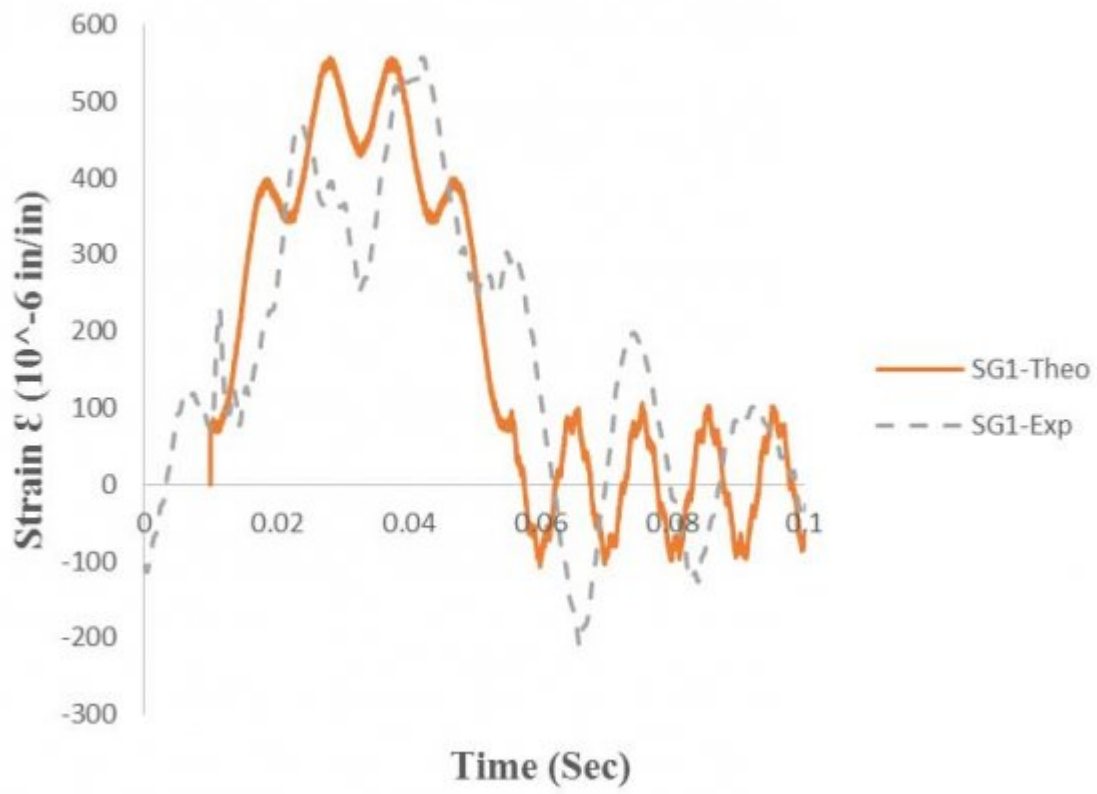
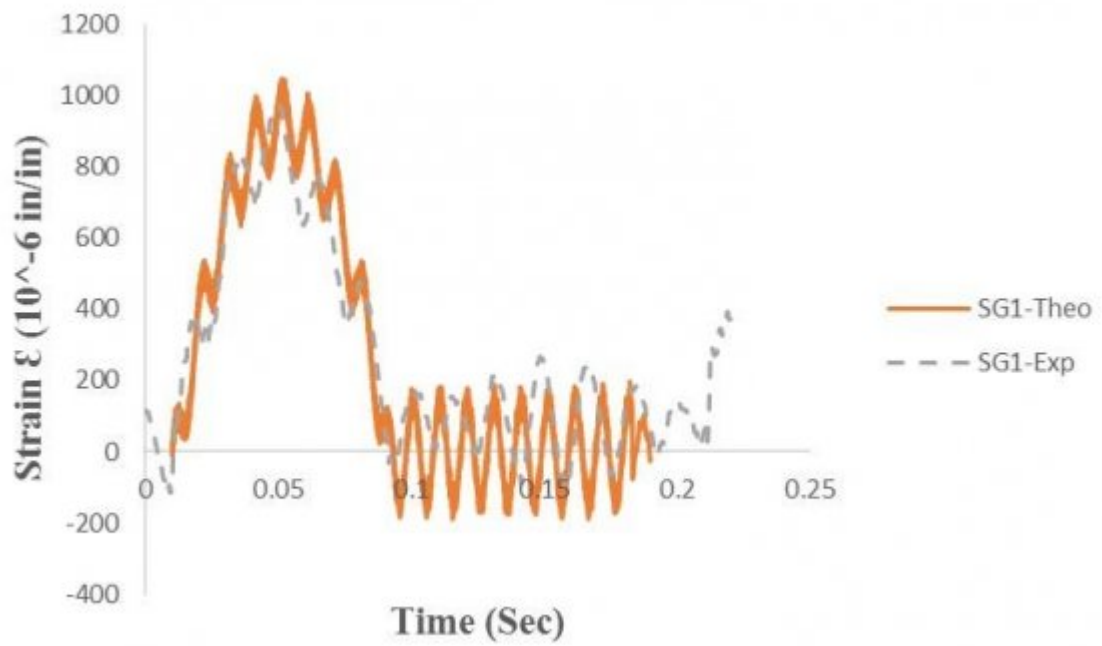
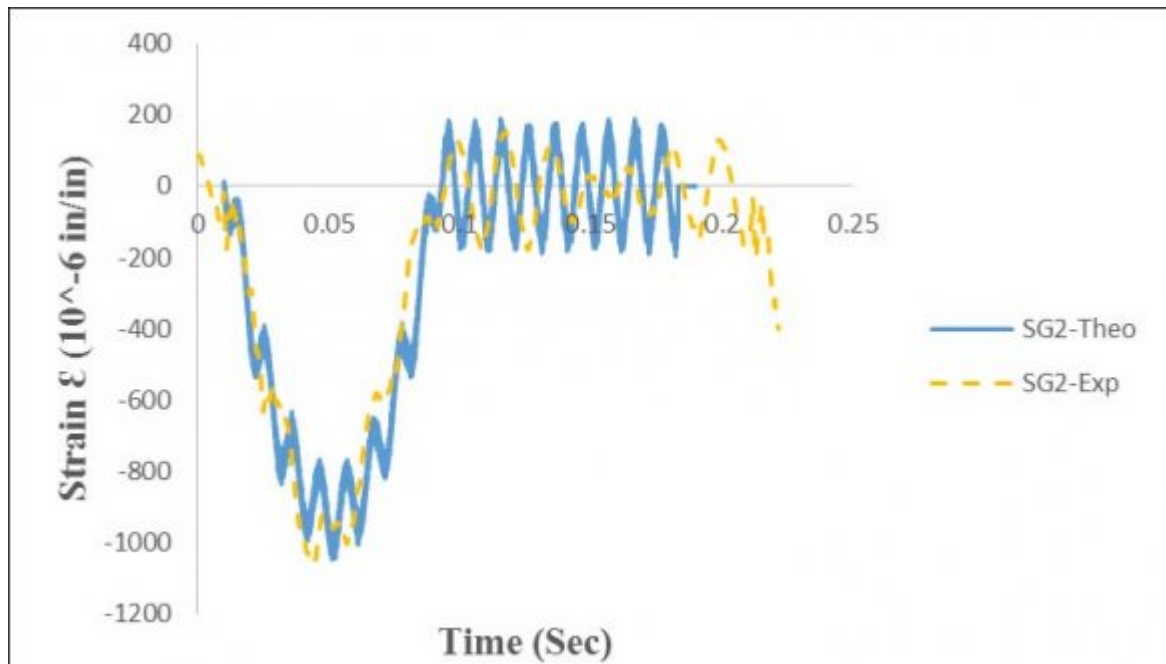


Figure 4:



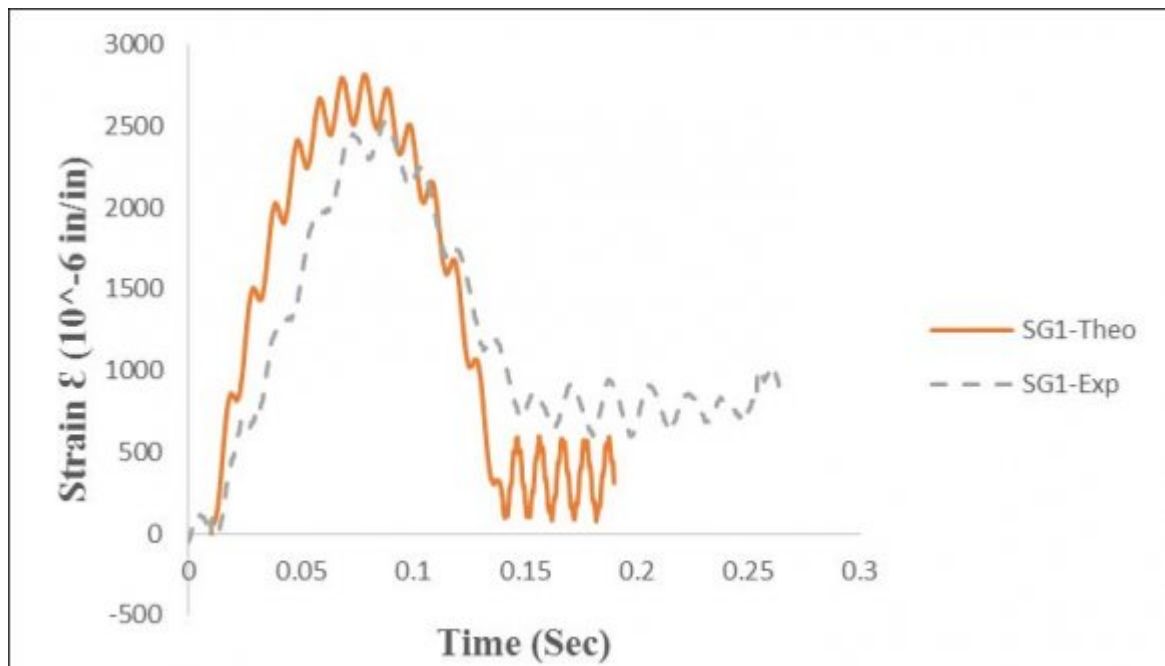
516

Figure 5: Figure 5 : 1 Figure 6 :



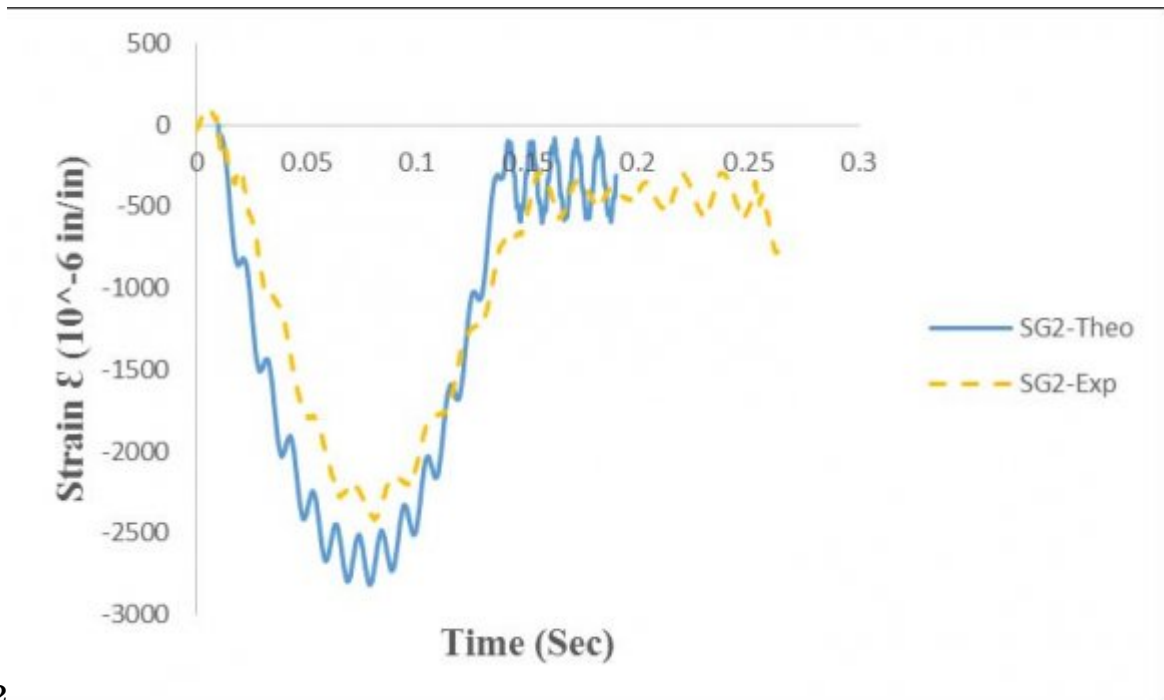
728

Figure 6: Figure 7 : 2 Figure 8 :



9310

Figure 7: Figure 9 : 3 Figure 10 :



12

Figure 8: Figure 12 :

1

between theoretical and experimental maximum moments at B for the cantilever beam impact tests

Test	Theoretical Max. Moment at B (kip-in.)	Experimental Max. Moment at B (kip-in.)
C1-1	9.4	10.8
C1-2	17.8	20.3
C1-3	37.7	38.1
C1-4	39.8	39.5

Figure 9: Table 1 :

2

Figure 10: Table 2 :

3

Figure 11: Table 3 :

4

Figure 12: Table 4 :

IV.

Figure 13: Table 5 :

157 found that the maximum curve-fitted acceleration value is inversely related to the mass of the impactor. <sup>1</sup>  
158 <sup>2</sup>

---

<sup>1</sup>© 2016 Global Journals Inc. (US) Elasto-Plastic Transient Dynamic Response of Tubular Section Steel Cantilever Beam under Impact Loading  
<sup>2</sup>© 2016 Global Journals Inc. (US)



- 
- 159 [E ()], E. *Global Journals Inc* 2016.
- 160 [Zeinoddini et al. ()] ‘Axially pre-loaded steel tubes subjected to lateral impacts: an experimental study’. M  
161 Zeinoddini, G A R Parkeb, J E Harding. *International Journal of Impact Engineering* 2002. (27) p. .
- 162 [Wen et al. ()] ‘Deformation And Failure Of Clamped Beams Under Low Speed Impact Loading’. H M Wen, T  
163 Y Reddy, S R Reid. *International Journal of Impact Engineering* 1995. 16 (3) p. .
- 164 [Ketter and Sherwood ()] *Modern Methods of Engineering Computation*, Robert L Ketter, Pravel Sherwood Jr  
165, P. 1969. McGraw-Hill Companies.
- 166 [Jones ()] ‘Quasi-static Analysis of Structural Impact Damage’. N Jones. *J. Construct. Steel Research* 1995.  
167 2016. (33) p. .
- 168 [Razzaq et al. (1983)] ‘Stability, Vibration and Passive Damping of Partially restrained imperfect columns’. Zia  
169 Razzaq, R T Voland, H G Bush, M M Mikulas. *NASA Technical Memorandum* October 1983. (85697) .
- 170 [Warburton ()] *The dynamical Behavior of Structures*, G B Warburton. 1976. Pergamon Press Ltd.